THE JOURNAL OF BIOLOGICAL CHEMISTRY VOL. 284, NO. 1, pp. 119–133, January 2, 2009

Structural Determinants of Antimicrobial and Antiplasmodial Activity and Selectivity in Histidine-rich Amphipathic Cationic Peptides*[S]

Received for publication, August 11, 2008, and in revised form, October 29, 2008 Published, JBC Papers in Press, November 4, 2008, DOI 10.1074/jbc.M806201200

A. James Mason[‡1], Wardi Moussaoui[§], Tamer Abdelrahman[¶], Alyae Boukhari[§], Philippe Bertani[‡], Arnaud Marquette[‡], Peiman Shooshtarizaheh[‖], Gilles Moulay[**], Nelly Boehm[‡‡], Bernard Guerold[‖], Ruairidh J. H. Sawers[§§], Antoine Kichler[**], Marie-Hélène Metz-Boutigue[‖], Ermanno Candolfi[¶], Gilles Prévost[§], and Burkhard Bechinger[‡]

*From the [‡]Université Louis Pasteur/CNRS, UMR7177, Institut de Chimie, 4 Rue Blaise Pascal, F-67070 Strasbourg, France, the [§]UPRES EA-3432 Institut de Bactériologie, Université Louis Pasteur-Hôpitaux Universitaires de Strasbourg, 3 Rue Koeberlé F-67000 Strasbourg, France, the [¶]UPRES EA-3950 Institut de Parasitologie et de Pathologie Tropicale de la Faculté de Médecine, Université Louis Pasteur, 3 Rue Koeberlé F-67000 Strasbourg, France, [‖]INSERM Unité 575, Physiopathologie du Système Nerveux, 5 Rue Blaise Pascal, F-67084 Strasbourg, France, **CNRS FRE 3087-Généthon, 1 Rue de l'Internationale, F-91002, Evry, France, [‡‡]INSERM Unité 666 and Service Central de Microscopie Electronique, Université Louis Pasteur, 11 Rue Humann, F-67085 Strasbourg, France, and the [§§]Department of Plant Molecular Biology, University of Lausanne, Biophore Building, CH-1015 Lausanne, Switzerland*

Designed histidine-rich amphipathic cationic peptides, such as LAH4, have enhanced membrane disruption and antibiotic properties when the peptide adopts an alignment parallel to the membrane surface. Although this was previously achieved by lowering the pH, here we have designed a new generation of histidine-rich peptides that adopt a surface alignment at neutral pH. *In vitro*, this new generation of peptides are powerful antibiotics in terms of the concentrations required for antibiotic activity; the spectrum of target bacteria, fungi, and parasites; and the speed with which they kill. Further modifications to the peptides, including the addition of more hydrophobic residues at the N terminus, the inclusion of a helix-breaking proline residue or using D-amino acids as building blocks, modulated the biophysical properties of the peptides and led to substantial changes in toxicity to human and parasite cells but had only a minimal effect on the antibacterial and antifungal activity. Using a range of biophysical methods, in particular solid-state NMR, we show that the peptides are highly efficient at disrupting the anionic lipid component of model membranes. However, we also show that effective pore formation in such model membranes may be related to, but is not essential for, high antimicrobial activity by cationic amphipathic helical peptides. The information in this study comprises a new layer of detail in the understanding of the action of cationic helical antimicrobial peptides and shows that rational design is capable of producing potentially therapeutic membrane active peptides with properties tailored to their function.

Antimicrobial peptides are being developed as a promising alternative for traditional antibiotic strategies (1) as bacteria increasingly threaten to win the antibiotic arms race. Knowledge of their mechanism of action can be used in the design of more powerful lead compounds; however, these mechanisms remain unclear, and debate continues as to the relative contributions of proposed pore formation or internal killing strategies (2). Cationic amphipathic α-helical peptides comprise an important group of antimicrobial peptides that have been studied quite extensively. Characteristically, these peptides comprise a high positive nominal charge segregated on one surface with a second surface formed of more hydrophobic residues. A number of models have been proposed describing their pore-forming activity (3), with a recent *in silico* study of the action of a magainin peptide (4) embracing the accumulated experimental evidence (*e.g.* see Refs. 5 and 6 and references therein). The computer simulations show that, above a threshold number of peptides, one peptide molecule becomes deeply embedded in the membrane interface. Subsequently, the membrane/water interface becomes unstable, and solvent molecules from the peptide-free interface are able to interact with suitably hydrophilic groups of the embedded protein, and a contiguous pore develops (4). Importantly, the peptides in the simulation retain an alignment approximately parallel to the membrane surface, and the acyl chains of lipids that interact with the peptides become strongly disordered, whereas the resulting pore is sufficient for cell contents to be released but importantly, since such behavior has been observed experimentally for magainin 2 (7), also allows passage of the peptide from one side of the membrane to the other (4). These observations agree well with our experimental biophysical studies of the membrane behavior of the cationic amphipathic antibiotic peptide pleurocidin (8), which has pore-forming capabilities (9) but has also been shown to inhibit intracellular processes (10). In particular, we used solid-state ^{15}N NMR methods on uniformly aligned samples to show that at peptide/lipid ratios where such pores are formed, the peptides adopt an orientation approximately par-

* This work was supported by Vaincre la Mucoviscidose Grant TG0501 (to B.B.) Inserm, Hôpitaux Universitaires de Strasbourg Grant PHRC3150 (to M.-H. M.-B.), and CNRS and Université Louis Pasteur (postdoctoral grants to A. J. M. and EA-3432). The costs of publication of this article were defrayed in part by the payment of page charges. This article must therefore be hereby marked "*advertisement*" in accordance with 18 U.S.C. Section 1734 solely to indicate this fact.

[S] The on-line version of this article (available at http://www.jbc.org) contains supplemental Table 1 and Figs. 1–7.

[1] To whom correspondence should be addressed: Pharmaceutical Science Division, King's College London, 150 Stamford St., London SE1 9NH, United Kingdom. Tel.: 44-207-848-4813; Fax: 44-207-848-4785: E-mail: james.mason@kcl.ac.uk.

allel to the membrane surface (8), in common with a range of other cationic helical antibiotic peptides (11–13). Furthermore, we used ^{2}H NMR of chain deuterated lipids in mixed model membranes to show that cationic pleurocidin strongly destabilizes anionic lipid acyl chains, in preference to zwitterionic lipids, indicating that such peptides are capable of causing local membrane disruption (8) and pore formation (14) while the membrane remains otherwise intact. When using model peptides to study this phenomenon, we showed that histidine-rich cationic amphipathic peptides, such as LAH4, have topologically dependent antibiotic activities (15, 16). The LAH4 helix adopts a trans-membrane alignment at neutral pH but flips to lie parallel to the membrane surface when the pH is lowered and the histidine residues become charged (17). At neutral pH, membrane disruption is weak, but at acidic pH, as determined by solid-state NMR studies of deuterium-labeled lipids in model membranes, the peptides strongly disrupt the acyl chains of the anionic lipid component of model membranes and also cause bacterial lysis (15). The antibiotic properties of LAH4 and related peptides therefore become enhanced at acidic pH when the peptide adopts a surface orientation in the membrane (15). We also noted that the model histidine-rich peptides had a greater membrane-destabilizing activity than the natural peptide pleurocidin (18). Considering our peptides in terms of the model described above, a histidine-rich peptide with enhanced membrane disruption properties should have excellent pore-forming activity, whereas its ability to undertake an intracellular killing strategy, through membrane translocation, may also be improved. To this end, we have designed and prepared histidine-rich peptides that adopt a surface orientation at neutral pH. These peptides all have excellent lipid-destabilizing capabilities in anionic membranes; however, their pore-forming capabilities, as determined by a dye release assay, varied considerably, indicating that pore formation may sometimes only be incidental to other bactericidal effects. We have evaluated the *in vitro* antimicrobial performance of the peptides and find them to be powerful antibacterial, antifungal, and antiplasmodial agents, whereas the toxicity of the peptides to human cells and *Plasmodium falciparum* can be related to further modifications to the peptide sequence and chirality, showing that rational design strategies have the potential to mold peptides for a range of applications.

MATERIALS AND METHODS

Peptide and Lipids—Tentagel S RAM Fmoc[2] resins were obtained from Rapp Polymere GmbH (Tübingen, Germany). The peptides (Table 1) were synthesized using standard Fmoc solid-state chemistry on a Millipore 9050 synthesizer or an Applied Biosystems 433A peptide synthesizer. In crude peptide preparations, a predominant peak was observed when analyzed by HPLC with acidified acetonitrile/water gradients. During HPLC purification, the main peak was collected, and the identity of the product was confirmed by matrix-assisted laser desorption ionization mass spectrometry. Peptides were lyophilized from 4% acetic acid to remove the trifluoroacetic acid counter ion. The lipids 1-palmitoyl-2-oleoyl-*sn*-glycero-3-phosphatidylethanolamine (POPE), 1-palmitoyl-2-oleoyl-*sn*-glycero-3-phosphatidylglycerol (POPG), 1-palmitoyl-2-oleoyl-*sn*-glycero-3-phosphatidylcholine (POPC), 1-palmitoyl-2-oleoyl-*sn*-glycero-3-phosphatidylserine (POPS), 1-palmitoyl$_{d31}$-2-oleoyl-*sn*-glycero-3-phosphatidylglycerol (POPG-d31), 1-palmitoyl$_{d31}$-2-oleoyl-*sn*-glycero-3-phosphatidylcholine (POPC-d31), 1-palmitoyl$_{d31}$-2-oleoyl-*sn*-glycero-3-phosphatidylserine (POPS-d31), and cholesterol were obtained from Avanti Polar Lipids, Inc. (Alabaster, AL) and used without further purification. All other reagents were analytical grade or better.

Circular Dichroism Experiments—Spectra were acquired on a Jasco J-810 spectrometer with samples maintained at 37 °C. Spectra were recorded from 250 to 190 nm using a spectral bandwidth of 1 nm and a scan speed of 100 nm/min. Peptides in 200 μl of phosphate-buffered saline (PBS) were added to 200 μl of trifluoroethanol to a final concentration of 0.5 mg/ml. Vesicles containing POPC/POPG (75:25) were prepared at a concentration of 5 mg/ml. 240 μl of lipid suspension was added to a 1-mm cuvette, and then 12 μl of peptide solution (2 mg/ml) was added and then thoroughly mixed such that a peptide/lipid molar ratio of 1:40 was maintained. Spectra were treated using Jasco spectra analysis software where a spectrum of the peptide-free solution/suspension was subtracted and, for spectra obtained for vesicles, means movement smoothing with a convolution width of 5 points was applied.

Sample Preparation for Solid-state NMR—For solid-state NMR, POPE/POPG-d31, POPC-d31/cholesterol, and POPC/POPS-d31/cholesterol were mixed at a molar ratio of 75:25, 100:30, and 70:30:30, respectively. A total of around 5 mg of lipids/sample were dissolved and mixed in chloroform and dried under rotor evaporation at room temperature. In order to remove all organic solvent, the lipid films were exposed to vacuum overnight. The films were then rehydrated with 5 ml of a suspension of peptide in 0.1 M Tris, 0.1 M KCl buffer at pH 7.5 at room temperature. For wide line ^{2}H NMR experiments, peptides were added at 2.5 mol %. The samples were briefly sonicated in a bath sonicator to improve exposure of all lipids to the peptide. Samples were subjected to five rapid freeze-thaw cycles for further sample homogenization and then centrifuged at 21,000 $\times$ *g* for 20 min at room temperature. Previous determination of a partitioning constant of 3.5×10^3 (16) for in-plane LAH4 and PC vesicles at pH 5 indicates that very little peptide will be free in solution after this process. The pellets, containing lipid vesicles and associated HALO derivatives, were transferred to Bruker 4-mm MAS rotors for NMR measurements. Lipid vesicles were also prepared in this way in the absence of HALO derivatives.

[2] The abbreviations used are: Fmoc, *N*-(9-fluorenyl)methoxycarbonyl; HPLC, high pressure liquid chromatography; POPE, 1-palmitoyl-2-oleoyl-*sn*-glycero-3-phosphatidylethanolamine; POPG, 1-palmitoyl-2-oleoyl-*sn*-glycero-3-phosphatidylglycerol; POPC, 1-palmitoyl-2-oleoyl-*sn*-glycero-3-phosphatidylcholine; POPS, 1-palmitoyl-2-oleoyl-*sn*-glycero-3-phosphatidylserine; POPG-d31, 1-palmitoyl$_{d31}$-2-oleoyl-*sn*-glycero-3-phosphatidylglycerol; POPC-d31, 1-palmitoyl$_{d31}$-2-oleoyl-*sn*-glycero-3-phosphatidylcholine; POPS-d31, 1-palmitoyl$_{d31}$-2-oleoyl-*sn*-glycero-3-phosphatidylserine; PBS, phosphate-buffered saline; CP, cross-polarization; MTT, 3-(4,5-dimethythiazol-2-yl)-2,5-diphenyltetrazolium bromide; FCS, fetal calf serum; IP, propidium iodide; MIC, minimal inhibitory concentration.

Static aligned samples were prepared using a procedure whereby a sublimable solid is co-dissolved with the lipids and peptide to aid alignment during dehydration and rehydration (19). 4 mg of HALO, carrying two ^{15}N-leucine labels at positions Leu-12 and Leu-14 was co-dissolved with POPE/POPG (75:25) or POPC/cholesterol (100:30) in chloroform at 2.5 mol %. The solvent was evaporated under a stream of nitrogen gas and redissolved in a solution of chloroform containing naphthalene. The molar ratio of naphthalene to lipid was 1:1. The solution was layered over 15 thin glass plates (9 × 22 mm; Marienfeld GmbH, Lauda-Königshofen, Germany), and the plates were then exposed to high vacuum overnight. The samples were rehydrated at 93% humidity and at 37 °C.

Solid-state NMR—^{2}H quadrupolar echo experiments (20) for samples containing POPG-d31 or POPC-d31 were performed at 46.10 MHz on a Bruker Avance 300 NMR spectrometer using a 4-mm MAS probe without rotation, spectral width of 200 kHz, and with recycle delay, echo delay, acquisition time, and 90° pulse lengths of 0.3 s, 42 μs, 2 ms, and 5 μs respectively. The temperature was maintained at 37 °C to keep the bilayers in their liquid-crystalline phase. During processing, the first 40 points were removed in order to start Fourier transformation at the top of the echo. Spectra were zero-filled to 8192 points, and 50-Hz exponential line broadening was applied. Smoothed deuterium order parameter profiles were obtained from symmetrized and dePaked ^{2}H NMR powder spectra of POPG-d31 or POPC-d31 using published procedures (21–23). ^{15}N cross-polarization (CP) spectra of static aligned samples were acquired at 40.54 MHz for ^{15}N on a Bruker Avance 400 NMR spectrometer equipped with a double resonance flat-coil probe. An adiabatic CP pulse sequence was used with a spectral width, acquisition time, CP contact time, and recycle delay time of 25 kHz, 10 ms, 800 μs, and 3 s, respectively. The ^{1}H $\pi/2$ pulse and spinal64 heteronuclear decoupling field strengths were 42 kHz. 40,960 scans were accumulated and the spectra were zero-filled to 4096 points, and 100-Hz exponential line broadening was applied during processing. Spectra were externally referenced to $^{15}NH_4Cl$ at 41.5 ppm.

Dye Release Assay—Large unilamellar vesicles loaded with calcein were prepared by mechanical extrusion. Three lipid mixtures, POPE/POPG (75:25), POPC supplemented with 40 mol % of cholesterol, and POPC/POPS (75:25) supplemented with 40 mol % cholesterol, were dissolved separately in chloroform/methanol. The solutions were dried and then hydrated in PBS buffer (50 mM, pH 7.4) with 50 mM of calcein ions (calcein disodium salt; Fluka, Switzerland) before undergoing several freeze-thaw cycles and then extrusion (11 times) through a 200-nm pore membrane (Avestin). The calcein-entrapped vesicles were separated from the dye solution by gel filtration on a Sephadex G-50 column (2.5 × 3.5 mm) (Sigma) loaded with PBS buffer (50 mM, pH 7.4) supplemented with 75 mM NaCl in order to compensate for the change in osmolarity induced by the presence of calcein molecules and Na^+ counter ions. The concentrations of the large unilamellar vesicle suspensions eluting from the column were determined by comparing 100% dye release from suspensions before and after the gel filtration step. A dilution factor of ~7 after gel filtration was usual. Calcein efflux measurements were performed on a Fluorolog 3-22 spectrometer (HORIBA Jobin-Yvon, Longjumeau, France). In a typical experiment, 10.5 μl of the large unilamellar vesicle solution (3 mg/ml) was added to 1.5 ml of PBS buffer (50 mM, pH 7.4) in a quartz cuvette and equilibrated for some minutes at 37 °C inside the spectrometer. 7 μl of peptide solution (2 mg/ml) were added into the cuvette while the sample was excited at λ_{exc} = 480 nm, and the intensity of fluorescence (I) was recorded at λ_{fluo} = 515 nm for about 10 min. A spectral bandwidth of 1 nm was used for both excitation and emission. The percentage of calcein released from the vesicles ($I_{\%}$) was calculated according to the formula, $I_{\%} = 100 \times (I - I_0)/(I_{max} - I_0)$, where I_0 represents the intensity of fluorescence before adding the peptide to the solution, and I_{max} is the maximum intensity observed after dissolving the vesicle with 10 μl of 10% Triton X-100. Care was taken to maintain constant I_{max} in order to allow quantitative comparison between the multiple recordings.

Antibacterial Assays—For details of strains tested, see the supplemental material. The antibacterial activities of the peptides were tested using a Mueller-Hinton Broth medium (Difco). Bacteria were first grown aerobically with vigorous shaking at 37 °C, and aqueous peptides solutions (10 μl) were incubated in a 96-well microplate with 100 μl of a mid-logarithmic phase culture of bacteria with a calculated starting $A_{620\,nm}$ of 0.001 (~2.5 × 10^5 colony-forming units/ml). Microbial growth was assessed by the increase of $A_{620\,nm}$ after an 18-h incubation at 37 °C, and the value of control cultures growing without peptide was taken as 100%. Each assay was performed in triplicate, and the antibacterial activity is evaluated with the minimal inhibitory concentration inhibiting 100% of bacterial growth (MIC100).

Scanning Electron Microscopy—Bacteria (*Escherichia coli* RSO2 and *Staphylococcus aureus* ATCC 52156) were grown to exponential phase ($A_{620\,nm}$ = 0.5) into 3 ml of Mueller-Hinton broth and then centrifuged at 6 °C at 5000 × *g* and further washed in distilled H_2O. The final bacterial pellet was fixed in 2.5% (v/v) glutaraldehyde in 0.1 M sodium cacodylate buffer at pH 7.4. The suspension was then applied to coverslips precoated with poly-L-lysine for scanning electron microscopy and kept in a hydrated chamber for cells to adhere for 2 h. Attached cells were rinsed in 0.1 M cacodylate buffer at pH 7.4, dehydrated in increasing concentrations of ethanol. The coverslips were mounted on stubs and sputter-coated with gold. Samples were examined in a Cambridge Stereoscan 360.

Antifungal/Yeast Assay—The following filamentous fungi strains were used: *Tricophyton mentagrophytes*, *Neurospora crassa*, and *Aspergillus fumigatus*. Spores at a final concentration 10^4 spores/ml were suspended in a growth medium containing potato dextrose broth (Difco, BD Biosciences Microbiology Systems) at half-strength, supplemented with tetracycline (10 mg/ml) and cefotaxime (0.1 mg/ml). Aliquots of peptide (10 μl) were incubated in microtiter plates with 90 μl of fungal spore cultures. Fungal growth was assessed microscopically after an appropriate incubation period (24 or 48 h at 30 °C). Similarly, yeast cells were precultured in a Sabouraud medium with starting absorbance of 0.001 at 620 nm. Two strains were tested: *Candida albicans* and *Candida tropicalis*. Growth of yeast was monitored and evaluated by measuring the

culture absorbance at 620 nm, using a microplate reader. Finally, MIC100 was calculated as the minimal concentration completely inhibiting cell growth.

Antiplasmodial Assay—Erythrocytic stages of *P. falciparum* were cultivated using the candle-jar technique using the chloroquine-sensitive strain 3D7 (24). The peptides, diluted in phosphate-buffered saline, were distributed on 96-well tissue culture plates with different concentrations. For each plate tested, three control wells were peptide-free, and each concentration was studied in triplicate. The blood samples were washed three times with a solution of RPMI 1640 (Invitrogen) supplemented with 25 mM HEPES (Sigma) and 25 mM $NaHCO_3$ (Sigma). The blood samples were then resuspended in the same supplemented culture medium. If necessary, a dilution was performed by adding uninfected O-positive-group erythrocytes (EFS-Alsace, France) to obtain a 1% parasite density and a hematocrit value of 2%. The plates were incubated for 4 days at 37 °C using the candle jar technique. The inhibition concentration was determined according to the effect of different peptide concentrations on the parasitemia, estimated in the 96-well test plate after 1, 2, 3, or 4 days. For the estimation of the parasitemia, light microscopy of a thin blood film stained with Giemsa was used. For IC_{50} calculation, an enzyme-linked immunosorbent assay was used for detection of pLDH secreted by *P. falciparum* similarly as described recently (25). Values for differing concentrations of peptides were plotted on a standard curve, and the IC_{50} value for each peptide was determined using linear regression analysis.

3-(4,5-Dimethythiazol-2-yl)-2,5-diphenyltetrazolium Bromide (MTT) Assay—Cytotoxicity was evaluated by performing the MTT (Sigma) assay (26). Dulbecco's modified Eagle's medium (Invitrogen) was supplemented with 2 mM L-glutamine, 100 units/ml penicillin, 100 μg/ml streptomycin, and 10% (w/v) of fetal calf serum (FCS; HyClone). 90,000 human fetal lung fibroblasts (MRC-5) or 120,000 SV40 transformed human fetal lung fibroblasts (MRC-5 V2) per well were plated in 24-well plates (Costar) 1 day before the assay. The cells were incubated with peptide solutions for 4 h in the presence or absence of 10% (v/v) FCS. Cells were incubated with 1% (v/v) Triton X-100 as a positive control (100% toxicity), whereas untreated cells were used as a negative control. The cell culture medium was then removed and replaced by serum-free Dulbecco's modified Eagle's medium (450 μl) and 50 μl of MTT (5 mg/ml in PBS), and the cells were incubated at 37 °C for 2 h. The medium was then removed, and 500 μl of DMSO was added to each well to dissolve the formazan crystals produced from the reduction of MTT by viable cells, and the absorbance was measured at 570 nm. The value reported for the EC_{50}, the concentration of peptide causing 50% toxicity, is based on nonlinear regression analysis of logarithmic serial dilution experiments performed in duplicate. Nine peptide concentrations, distributed above and below the expected EC_{50}, were tested. For each combination of peptide and cell line, the relationship between toxicity and peptide concentration was modeled using a logistic curve of the following form,

$$\text{Toxicity} = \frac{50 \times (1 + e^{b - g \times \text{EC}_{50}})}{1 + e^{b - g \times \text{concentration}}} \qquad \text{(Eq. 1)}$$

TABLE 1

The sequences of histidine-rich peptides used in this study

Positively charged residues at acidic pH are marked in boldface type, and D-amino acids are in italic type, whereas the positions of ^{15}N-labeled amino acids incorporated for aligned solid-state NMR measurements are underlined. The peptides are all C terminally amidated, contributing one extra positive charge overall.

Peptide	Sequence	Sequence length	Nominal charge at pH 7.2
LAH4-L1	**KK**ALLA**H**AL**H**LLALLAL**H**LA**H**AL**KK**A	26	+5
LAH4-L1-IP	LALAL**KH**AL**HK**ALLLA**KH**LA**HK**LALA	26	+5
HALK	**KK**ALL**KH**AL**HK**LALLA**KH**LA**HK**L**KK**A	26	+9
HALO	**KK**ALL**OH**AL**HO**LALLA**OH**LA**HO**L**KK**A	26	+9
HALO-2	ALALL**OH**AL**HO**LALLA**OH**LA**HO**LALA	26	+5
HALO-F	FF**KK**L**OH**AL**HO**LALLA**OH**LA**HO**L**KK**A	26	+9
HALO-P8	**KK**ALL**OH**PL**HO**LALLA**OH**LA**HO**L**KK**A	26	+9
HALO-P8F	FF**KK**L**OH**PL**HO**LALLA**OH**LA**HO**L**KK**A	26	+9
D-HALO-rev	*AKKL**OH**AL**HO**ALLAL**OH**LA**HO**LLA**KK***	26	+9
D-HALO-P8F-rev	*AKKL**OH**AL**HO**ALLAL**OH**LP**HO**L**KK**FF*	26	+9
KALP	G**KK**LALALALALALALALAL**KK**A	23	+5

where b, g, and EC_{50} are fitted parameters. Initial estimates were obtained by inspection of data plots and then optimized iteratively using the nonlinear least squares function in the R statistics package (R Foundation for Statistical Computing). S.E. and significance levels were taken from the R output. Analysis of variance of the EC_{50} point estimates was performed to investigate peptide and cell line differences.

Flow Cytometry—MRC5 and MRC5-V2 cells were washed twice with PBS, harvested in a trypsin-EDTA/PBS solution (1:1), and finally stained with propidium iodide (IP) and Annexin V-fluorescein isothiocyanate as described by BD Pharmingen. Ten thousand IP-negative MRC5 and MRC5-V2 cells were then analyzed by flow cytometry (FACSCalibur; BD Biosciences) for Annexin V-fluorescein isothiocyanate staining.

RESULTS

Peptide Design—Since LAH4 and its derivatives have much improved antibiotic activity at acidic pH when the peptide adopts an in-plane orientation with respect to the membrane (15), we designed peptides that retained the essential elements of the LAH4 peptides, namely the α-helicity and positioning of the histidine residues, while incorporating structural features that would provoke an in-plane orientation at neutral pH (Table 1). In a previous study (15), we prepared a series of LAH4 isomers that differed in the angle subtended by the histidine residues when the peptide adopts an α-helical conformation, and hence some consideration is required in selecting one of these peptides as the starting point for the new generation of peptides. Although early studies of lytic amphipathic helices showed that increasing the hydrophilic angle led to a reduction of hemolytic activity (27), our own experiments using LAH4 isomers in mixed membranes containing zwitterionic lipids, anionic lipids, and cholesterol revealed an intermediate angle, of between 80 and 100°, to cause the most effective membrane disruption (28). A detailed investigation of the effect of altering the charged angle in magainin 2 (29) found that this led to a perturbation of the peptide hydrophobic moment, and hence this was compensated for in the design of the magainin analogues. Increases in the charged angle of these mutant peptides led to an increase in the membrane activity in terms of dye release from liposomes as well as in antimicrobial and hemo-

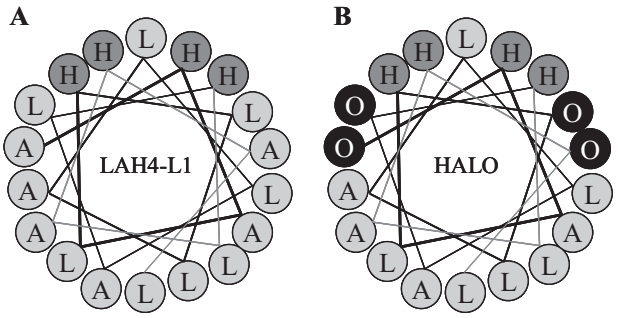

FIGURE 1. **Helical wheel representation of LAH4-L1 (*A*) and HALO (*B*) showing location of the hydrophobic residues (*light gray*), histidine residues (*dark gray*), and positively charged ornithine residues (*black*).**

lytic activity (29). However, the two peptides with reduced angles of 80 and 100° were shown to have a much reduced binding affinity, perhaps as a result of balancing the hydrophobic moment. Consequently, although these peptides were apparently less active when analyzed as a function of overall concentration, the peptides with reduced angles were in fact shown to be more effective at disrupting membranes composed of zwitterionic POPC or mixed POPC/POPG when the peptide bound to the membrane is considered (16, 29). In a more recent study where the hydrophobic moment was not balanced, amphipathic α-helical Hept peptides with charged angles of 80 or 100° were found to be far more effective at disrupting POPC or POPC/POPG membranes than peptides with larger angles, and, indeed, the peptide 1,5-Hept, with an angle of 80°, showed some selectivity between POPC and POPC/POPG membranes at lower peptide to lipid ratios of 64:1 and 32:1 (30). Enhanced membrane disruption and selectivity for anionic lipids in mixed membranes are attractive properties when looking to design peptides that act on the membranes of bacteria or transformed eukaryotic cells, and hence LAH4-L1 was used in the present work as the starting point for the new generation of peptides, since it is one of the two LAH4 isomers that cause the most effective disruption of anionic membranes, even in the presence of sterols (28). It has a charged angle of 80°, which may afford some selectivity for anionic lipids in the target membranes, whereas the relatively acute charged angle adopted in an ideal helix allows further charged residues to be added while maintaining amphipathicity (Fig. 1). To force an in-plane orientation, we either moved or added four positively charged residues to the center of the primary peptide sequence. The charges on either lysine or ornithine residues are located somewhat further from the helix backbone than those of histidine when charged, and their positioning in the helical wheel is intended to allow interaction between the histidine side chains and the lipid head groups; however, the positioning of the additional charged residues in the helical wheel does alter the angle described by such residues and could be a cause of altered selectivity between zwitterionic and anionic membranes in the new generation of peptides. In the case of HALO or HALK, the four additional charged residues increase the overall charge of the peptide from +5 to +9 at neutral pH, and the lysine residues at the C and N termini are retained, in contrast to HALO-2 and LAH4-L1-IP (an isomer of LAH4-L1), where the strong positive charges at the termini are absent.

Further modifications were introduced to the HALO sequence to obtain a greater understanding of the mechanism of both antibiotic activity and toxicity toward eukaryotic cells. Unlike naturally occurring antimicrobial peptides, the designed HALO peptides are almost symmetrical, with an even distribution of hydrophobic and charged residues throughout the length of the peptide. Naturally occurring antimicrobial cationic helical peptides often have hydrophobic residues clustered at the N terminus, and these might be expected to induce a slight tilt of the helix from a parallel surface alignment. To understand the effect of this common structural feature, a peptide was designed (HALO-F; Table 1), where two phenylalanine residues were introduced at the N terminus, with the lysines being shifted two residues toward the C terminus. Previous structure-activity studies of the naturally occurring histidine-rich antimicrobial peptide piscidin 1 demonstrated that improved selectivity between bacterial targets and host red blood cells could be obtained by introducing a proline residue at position 8 (31). The induced conformational flexibility and the optimal length of the second, C-terminal, α-helix were proposed to be the critical factors in conferring this selectivity (31). We therefore prepared a HALO derivative (HALO-P8; Table 1), where, analogously, we introduced a proline residue in position 8.

Finally, since incorporation of D-amino acids in both natural (32) and designed (33, 34) antibiotic peptide sequences increases the robustness of the peptides when challenged by either serum (33) or enzymatic degradation (32), we also prepared two peptides where the peptides were synthesized using D-amino acids as building blocks. One peptide was a version of HALO where the sequence had been reversed (D-HALO-rev), whereas the other also incorporated the phenylalanine and proline residues discussed above (D-HALO-P8F-rev).

Antimicrobial and Antiplasmodial Activity of HALO Peptides—The antibacterial and antifungal/anticandidal activities of the HALO peptides are shown in Table 2. The peptides possess broad range antibiotic activity against a variety of Gram-positive and -negative bacteria comprising both drug-sensitive and drug-resistant strains (see supplemental material for details). In particular, HALO peptides demonstrate powerful antibiotic activity against *E. coli*, *S. aureus*, and multidrug-resistant *Pseudomonas aeruginosa*, bacteria that constitute common human pathogens. The HALO peptides had somewhat lower activity against *S. aureus* that has acquired resistance to methicillin or *Enterococcus faecalis*. In a killing curve analysis (supplemental Fig. 1), for each of six bacterial strains, bacteria challenged with HALO at between 2 and 8 times the MIC were eliminated within 2 h.

Many cationic antimicrobial peptides are rich in lysine residues. For the HALO peptides, we used ornithine residues in place of lysine to see if using an uncommon amino acid would confer some advantage to the antibacterial activity. To test this hypothesis, we also prepared peptides where lysines were incorporated in place of ornithine residues (HALK and LAH4-L1-IP; Table 1). These peptides were observed to have antibiotic activities almost identical to those of their respective ornithine-rich analogues (HALO and HALO-2) (data not shown). We were able to conclude that the choice of lysine or ornithine residues,

TABLE 2

The antibacterial, antifungal, and antiplasmodial activity of selected HALO peptides against selected organisms (further information on bacterial strains can be found in the supplemental material)

HALO was also shown to be active against nonpathogenic strains of the gram-positive bacteria *Bacillus megaterium*, *Rhodococcus equi*, and *Micrococcus luteus* at comparable concentrations (6.25 μM or better) and against the gram-negative bacteria *Acinetobacter baumanii* and *Stenotrophomonas maltophilia* (11.2 μM).

Cell type	Gram stain	MIC					
		HALO	HALO-2	HALO-F	HALO-P8	D-HALO-rev	D-HALO-P8F-rev
		μM					
Bacteria							
E. coli (RSO2)	−	2.8	5.6	2.8	5.6	2.8	1.4
S. aureus (ATCC 52156)	+	>11.2	5.6	4.2	11.2	4.2	4.2
S. aureus (MET^R)	+	>11.2	22.4	11.2	>11.2	11.2	>11.2
P. aeruginosa	−	11.2	>22.4	2.8	4.2	4.2	2.8
E. faecalis	+	5.6	11.2	4.2	11.2	11.2	>11.2
Fungi							
N. crassa		3.125		3.125	3.125	1.563	
A. fumigatus		50[a]		50[a]	50[a]	50[a]	
T. mentagrophytes		25		25	12.5	12.5	
C. albicans		25		25	50	25	
C. tropicalis		0.75		1.5	0.75	0.75	
Parasite (IC_{50})							
P. falciparum		11.7			17	0.1	10.3
Red blood cells (HC_{50})		179.2	<5.6	<5.6	89.6	716.8	>65.2

[a] Only 90% inhibition achieved at this, the highest concentration tested. HC_{50} represents the peptide dose that causes 50% hemolysis of red blood cells *in vitro*.

in this study, did not affect the behavior of the peptides, and HALK and LAH4-L1-IP were therefore not studied any further.

Importantly, despite the range of modifications made to the primary sequences, the activities of the HALO family of peptides, with the same +9 nominal charge, were similar against all bacteria tested. HALO-2 (and LAH4-L1-IP), however, with a nominal charge of only +5, had consistently lower activity against the majority of strains tested and was therefore not included in subsequent tests. D-HALO-P8F-rev was prepared in response to the data described in the toxicity and biophysical studies below. Interestingly, this peptide was observed to have a small but significant advantage over the other members of the HALO family when challenging certain bacteria (Table 2).

When tested against a selection of fungi or *Candida* spp., the HALO peptides again showed interesting antimicrobial activity (Table 2). There was considerable variation in peptide antimicrobial activity between differing fungi and even between species of *Candida*. The HALO peptides were active at between 1.5 and 3.2 μM when challenging *N. crassa* but were rather less active against *T. mentagrophytes* and were only able to inhibit *A. fumigatus* at 90% at the maximum concentration tested (50 μM). Similarly, the HALO peptides were active against *Candida tropicalis* at very low concentrations (0.75 μM) but had only modest activity against *C. albicans* (25 μM). Again, there was very little variation in activities among the HALO peptides, indicating that the modifications to the HALO sequence did not have major effects on the antimicrobial activity.

Finally, the diverse nature of the potential therapeutic targets of the HALO peptides is highlighted by their activities against *P. falciparum* (Table 2), the eukaryotic parasite that causes malaria, cultured in erythrocytes. The four HALO peptides tested all demonstrate antiplasmodial activity at concentrations below that which causes significant lysis of red blood cells, whereas HALO was also capable of eliminating 98% of parasites. Interestingly, D-HALO-rev was the most active peptide by more than 2 orders of magnitude and was also the least hemolytic, with the concentration causing 50% inhibition of *P. falciparum* more than 7000 times lower than that which causes 50% lysis of red blood cells. Furthermore, although, as discussed below, D-HALO-rev is also the most toxic of the HALO peptides to fibroblasts, there remains a 2-order of magnitude difference between the concentrations that cause *P. falciparum* inhibition and fibroblast toxicity. This difference and the high antiplasmodial activity of the peptide at low concentration may make it an attractive candidate for future development of antimalarial treatments.

Cellular Toxicity of Histidine-rich Peptides—Modifications to the HALO sequence did, however have important consequences when the toxicity of the peptides to erythrocytes (Table 2) and human lung fibroblasts (Table 3) was assessed. The HALO peptides can be divided into two groups when assessing their toxicity against human erythrocytes. The first group, containing HALO, HALO-P8, D-HALO-rev, and D-HALO-P8F-rev, are characterized by low toxicity where the EC_{50} for red blood cell lysis is greater than 10 times the MIC for *E. coli* (Table 2); the second group, including HALO-F and HALO-2, are toxic to erythrocytes with an EC_{50} around or below the same concentration as the MIC for *E. coli*.

When human lung fibroblasts (MRC5) are challenged with helical peptides in the presence of fetal calf serum, only those peptides that are designed to adopt an in plane orientation at neutral pH are toxic (Table 3), the EC_{50} for trans-membrane oriented KALP (35) and LAH4-L1 being superior to the maximum peptide concentration tested (Table 3, top). In contrast, all of the HALO peptides are toxic in the range tested (Table 3, Expt.2/3). However, within the family of HALO peptides, there is considerable variation in toxicity (Table 3, middle); HALO and HALO-F are characterized by an EC_{50} (51.2 ± 4.9 and 47.3 ± 3.7 μM, respectively) against MRC5 cells in the presence of serum of more than 10 times that of the MIC for *E. coli*, whereas HALO-P8 has further reduced toxicity (EC_{50} = 99.1 ± 10.0 μM). Interestingly, the left-handed helical peptide, D-HALO-rev (EC_{50} 19.9 ± 7.6 μM), is rather more toxic to MRC5 cells than the α-helical HALO in the presence of serum, despite the situation being reversed when considering their toxicities to erythrocytes.

TABLE 3

Toxicity study of the model peptides as determined by an MTT assay

Human lung fibroblasts (MRC5) and SV40 virus-transformed fibroblasts (MRC5-V2) were challenged in the presence or absence of FCS. Results from three separate experiments are shown, one comparing HALO with peptides that adopt trans-membrane orientation at neutral pH (Expt. 1), one comparing peptides within the HALO series (Expt. 2), and a further experiment highlighting the characteristics of D-HALO-P8F-rev (Expt. 3). The selectivity index is the value for the MRC5 cells divided by that obtained for the MRC5-V2 cells in the corresponding environment. EC_{50} represents the peptide dose that kills 50% of the fibroblasts *in vitro*.

Peptide	EC_{50} (μM)				Selectivity index	
	MRC5	MRC5 (FCS)	MRC5-V2	MRC5-V2 (FCS)	Without FCS	With FCS
Expt. 1						
KALP	>228.0	>228.0	>228.0	>228.0	1	1
LAH4-L1	>184.2	>184.2	13.3 ± 2.1	>184.2	>13.8	1
HALO	38.0 ± 2.9	56.1 ± 5.0	26.5 ± 2.0	50.2 ± 5.1	1.43	1.12
Expt. 2						
HALO	48.8 ± 3.3	51.2 ± 4.9	21.6 ± 1.2	37.3 ± 3.8	2.26	1.37
HALO-F	39.9 ± 3.7	47.3 ± 3.7	12.4 ± 0.4	36.9 ± 0.4	3.22	1.28
HALO-P8	89.1 ± 10.6	99.1 ± 10.0	36.6 ± 2.6	60.4 ± 4.4	2.43	1.64
D-HALO-rev	30.0 ± 2.8	19.9 ± 7.6	14.6 ± 1.0	23.7 ± 2.5	2.05	0.84
Expt. 3						
HALO-F	17.8 ± 1.7	56.7 ± 3.9	14.4 ± 1.4	34.9 ± 2.8	1.24	1.62
HALO-P8	48.7 ± 5.0	117.1 ± 6.7	38.3 ± 3.5	66.3 ± 7.4	1.27	1.77
D-HALO-rev	19.5 ± 1.1	41.9 ± 4.5	20.9 ± 2.6	31.8 ± 3.3	0.93	1.32
D-HALO-P8F-rev	20.5 ± 1.3	57.9 ± 2.9	18.3 ± 1.9	39.6 ± 3.2	1.12	1.46

We have previously shown that LAH4, its derivatives, and pleurocidin disrupt anionic lipids preferentially in mixed membranes (8, 15, 27). This increased affinity for anionic lipids may have further consequences when considering interactions between histidine-rich peptides and eukaryotic cells. Anionic lipids are not normally exposed on the surface of eukaryotic cells, but cationic peptides do display selective toxicity against transformed eukaryotic cell lines over healthy cells (36–38), and this property has also been proposed to be due to a higher proportion of anionic lipids in the membranes of cancer cells (39). In particular, phosphatidylserine is often exposed at the membrane surface of a variety of pathological cells (40), including those of human tumor cells (41), and is a prominent hallmark of apoptotic cells. MRC5-V2 cells are human lung fibroblasts (MRC5) that have been transformed with the SV40 virus (42). Binding of fluorescently labeled Annexin V can be used to quantify the amount of phosphatidylserine presented on the cell surface. The binding pattern of Annexin V to MRC5 and MRC5-V2 cells is markedly different when compared with the normal background fluorescence associated with each cell type. Flow cytometry analysis reveals that the shift to higher fluorescence intensity observed for transformed MRC5-V2 cells upon binding of Annexin V is much greater than that for MRC5 cells, confirming the enrichment of phosphatidylserine in the external leaflet of MRC5-V2 cell membranes following transformation (see supplemental material). LAH4-L1 is only toxic to transformed fibroblasts; however, this selectivity is only observed when the cells are challenged in the absence of serum (Table 3, top). In contrast, HALO displays considerable toxicity against transformed human lung fibroblasts even in the presence of serum. Although caution should be taken when comparing peptide toxicity against cells from differing cell lines and passages, since this is a source of considerable variation, an analysis of variance indicates that the peptides in the HALO family have activity against the transformed MRC5-V2 cells that surpasses that against the normal MRC5 fibroblasts (mean EC_{50} MRC5 = 50.0 μM, MRC5-V2 = 32.5 μM $p = 0.025$). The selectivity index given in Table 3 gives an indication of this advantage and reveals that, in the presence of serum, HALO-P8 has the greatest selective advantage against the transformed fibroblasts. Considering the data as a whole, the presence of serum reduces the toxicity of the peptides (mean EC_{50} without FCS, 30.9 μM; with FCS, 51.6 μM; $p < 0.01$). D-HALO-rev and HALO-F are the most toxic peptides to both cell types irrespective of the culture conditions. Finally, having observed these toxicity patterns and the biophysical data described below, a further peptide was prepared that incorporated the toxic promoting phenylalanine and D-amino acid motifs in addition to the toxic preventing proline at position 8 to see whether a peptide with intermediate properties would result. Indeed, this peptide, D-HALO-P8F-rev, proved to have intermediate toxicity to both MRC5 and MRC5-V2 cells (Table 3, bottom), which, coupled with its robust activity against bacteria and low hemolysis, makes this peptide an attractive candidate for further development.

Scanning Electron Microscopy—Images of *E. coli* RSO2 and *S. aureus* ATCC 52156 were obtained using scanning electron microscopic techniques. Images were obtained for each bacterial species in the absence (Fig. 2, *A* and *F*) and presence (Fig. 2, *B–E* and *G–J*) of incubation for 30 min with D-HALO-P8F-rev. For *E. coli*, the first evidence of an effect of the peptide on the bacteria is observed at or slightly above the MIC (Fig. 2*C*). Below the MIC, the bacteria appear unaffected by the peptide challenge (Fig. 2*B*). Between the MIC and 4 times the MIC (Fig. 2, *C* and *D*), the bacteria become increasingly deformed as the concentration of peptide is increased. The deformation is quite pronounced at 4 times MIC, a bactericidal concentration, yet no lysis or loss of cell contents is apparent (Fig. 2*D*). At the highest peptide concentration tested (8 times MIC; Fig. 2*E*), although the bacterium retains its rodlike shape, the surface of the bacterium appears contorted, and the first evidence of leakage of cell contents is observed in the form of rough or irregularly stained material obscuring the cell surface. For *S. aureus*, even quite low concentrations (one-fourth MIC) are capable of causing some deformation of the cell in the form of membrane blebs (Fig. 2*G*). These blebs become more prevalent when the peptide is added at the MIC (Fig. 2*H*), although the bacteria appear to remain intact. At still higher concentrations (2 times

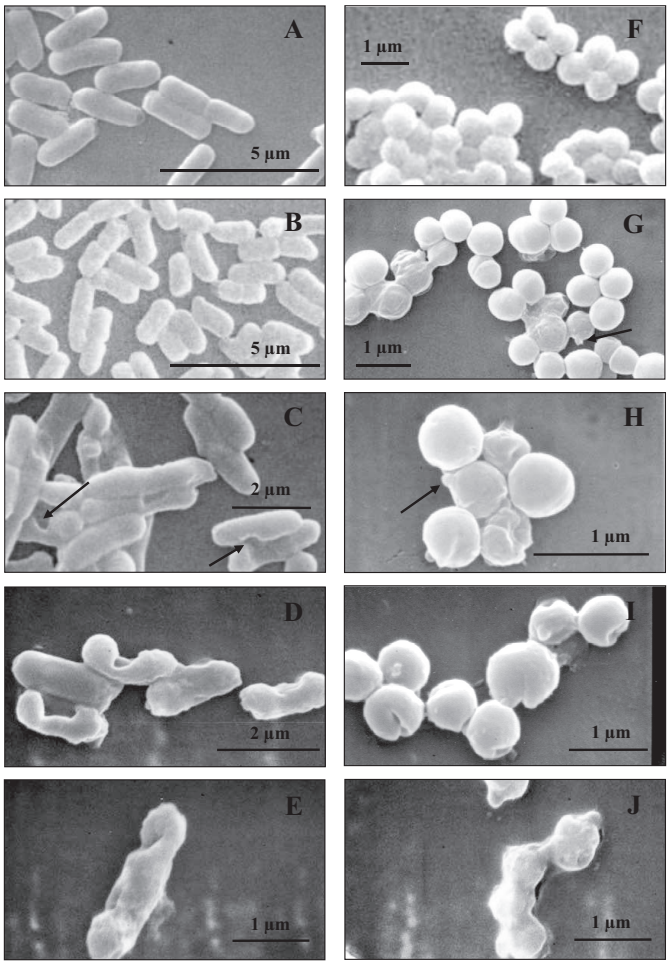

FIGURE 2. **Scanning electron micrographs of *E. coli* RSO2 (*A–E*) and *S. aureus* ATCC 52156 (*F–J*) incubated for 30 min with increasing amounts of the antimicrobial peptide D-HALO-P8F-rev.** For *E. coli* RS02, *A* shows peptide-free medium, whereas *B–E* contain peptide at 0.5, 2, 4, and 8 times the MIC. For *S. aureus* ATCC 52156, *F* shows peptide-free medium, and *G–J* contain peptide at 0.25, 1, 2, and 4 times the MIC.

MIC), the bacteria are affected by quite deep invaginations of the outer cell surface (Fig. 2*I*). Finally, at the highest peptide concentration tested (4 times MIC; Fig. 2*J*), the first evidence of the leakage of cell contents is observed. Therefore, when challenged by the most potent antibacterial peptide, both *E. coli* and *S. aureus*, representatives of Gram-negative and Gram-positive bacteria, respectively, respond similarly in that the peptide induces clear alterations in the morphology of the bacteria surface at inhibitory and bactericidal concentrations, but only at the most elevated concentrations is any direct evidence of leakage of cell contents observed.

Design of Biophysical Experiments—A general problem affecting biophysical studies of antimicrobial peptides is the choice of peptide concentration for each technique. Although the MIC for each combination of peptide and bacteria is known, the actual amount of peptide that reaches the bacterial cell membrane(s) is yet to be quantified. Estimates of the expected peptide/lipid ratio in the target membrane that are based on MIC values and the bacterial membrane surface area have suggested that as many as ~100 peptides could be present for each lipid molecule, although the true value is probably much lower, since the peptides may also bind to lipopolysaccharides, peptidoglycan, teichoic acid, or other components of the cell envelope (43). Furthermore, peptide/lipid supramolecular assemblies display considerable morphological plasticity, depending on the peptide concentration and lipid composition, with membranes remaining in a lamellar phase at low peptide concentrations but giving way to bicelles or even micelles as the peptide concentration is increased (44). In this and previous studies (8, 13–15), therefore, we have selected conditions for the biophysical studies where peptides are present at the lowest peptide/lipid ratio that will provoke an event in the membrane that might be expected to lead to bacterial cell death or where differences in peptide activity can be observed by the selected technique. Such events include calcein dye leakage induced by the naturally occurring antimicrobial peptide, pleurocidin, which is around 30% at a peptide/lipid ratio of 1:40 (45) or the formation of disordered toroidal pores observed *in silico* at peptide/lipid ratios of 1:32 (4). Solid-state NMR methods are sensitive to peptide-induced lipid chain disordering, as observed in such pores, at peptide/lipid ratios of between 1:59 (1.7 mol %) and 1:40 (2.5 mol %) in the present study. However, dye release experiments in the present studies were performed at peptide/lipid ratios of 1:9, since the HALO series of peptides could only induce leakage at these elevated levels.

Secondary Structure—CD spectra were acquired for samples dissolved in the helix-promoting solvent 50% trifluoroethanol, and these spectra were analyzed using the CDPro software suite (46) (see supplemental material). HALO, HALO-2, and HALO-F were determined to have average helical contents of >90%, whereas HALO-P8, containing a helix-breaking proline (47) residue at position 8, has reduced helical content. This corresponds to a loss of one single turn of helix in the peptide, presumably around Pro-8. The D-HALO-rev peptide adopts a left-handed helical conformation.

HALO and HALO-F adopt rather similar α-helical structures in a POPC/POPG model membrane environment, although there is less helix than in the 50% trifluoroethanol environment. HALO-P8 appears to have reduced helical content when compared with the HALO or HALO-F sequences, but the variation in the helical content values determined by the three programs in the CDPro suite means that this difference is not sufficiently significant, reflecting the quality of the spectra obtainable in this more experimentally challenging environment.

Dye Release Assay—The ability of the HALO peptides to induce pore formation, in model membranes composed of a variety of lipids, was assessed using a calcein dye release assay (Fig. 3). Interestingly, although the HALO derivatives all showed very similar antibacterial and antifungal activities, their abilities to promote dye release and hence induce pore formation were diverse. The dye release activities, at a peptide/lipid ratio of 1:9, of all of the HALO peptides were poor to modest for all three membrane compositions tested, with the exception of HALO-F. This is despite the fact that rather high peptide/lipid ratios were used. For comparison, in recent studies of the LAH4 peptides performed under the same conditions, between 40 and 90% dye release was observed with peptide/lipid ratios between 1:250 and 1:100 (48), whereas dye release induced by HALO

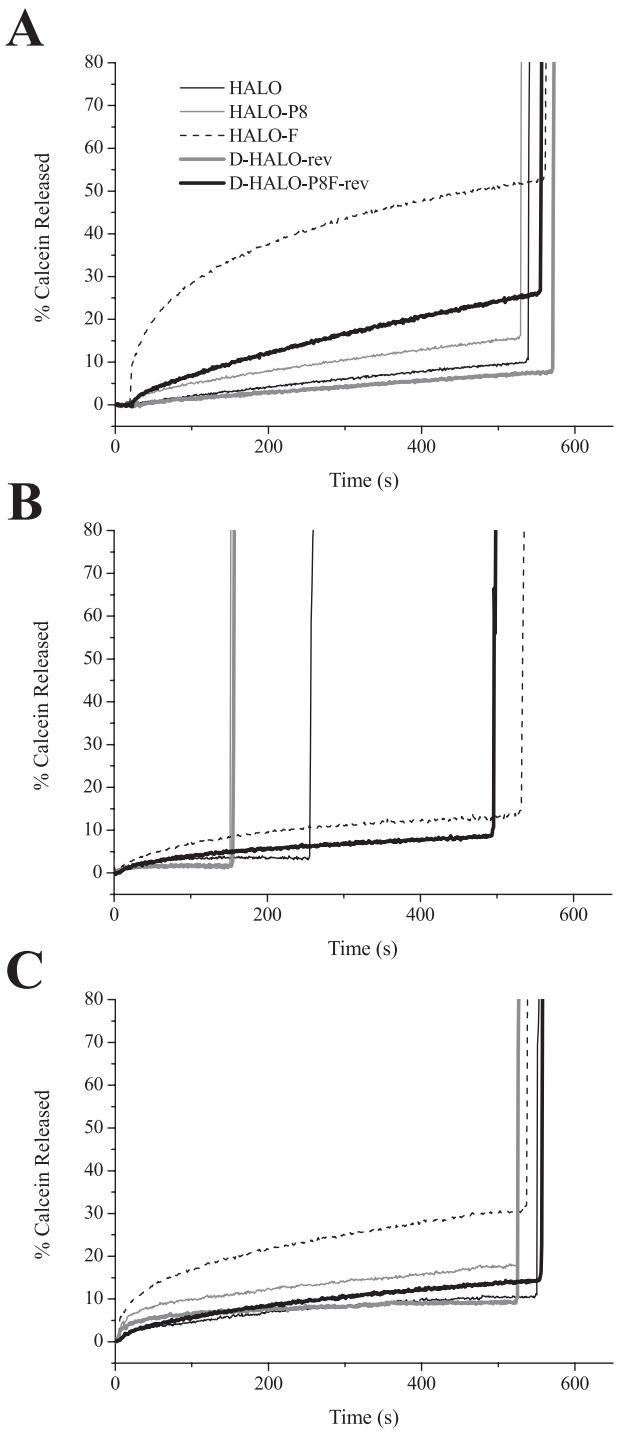

FIGURE 3. **Comparison of pore formation in POPE/POPG (*A*), POPC/cholesterol (*B*), or POPC/POPS/cholesterol (*C*) liposomes, assessed by monitoring the release of fluorescent calcein from large unilamellar vesicles when challenged with HALO and derivatives.** The experiment was performed at 37 °C and pH 7.4. Triton X-100 was added to terminate the experiment and to allow quantification of 100% calcein release.

peptides at such levels was negligible. Each of the HALO peptides, although not perfectly symmetrical in terms of its primary sequence, is well balanced around the center of the peptide with charged and hydrophobic residues equally distributed throughout the length of the sequence and at the N and C termini (Table 1). In contrast, HALO-F has two hydrophobic phenylalanine residues located at the extreme of the N terminus, a feature that would alter the balance between hydrophobic and charged resides between the N- and C-terminal segments of the primary sequence. HALO-F is the most effective peptide at challenging all three model membranes and causing dye release. In particular, its enhanced pore formation activity can be seen when challenging liposomes comprising anionic lipids (Fig. 3, *A* and *C*), and it clearly behaves rather differently from the other peptides when challenging POPE/POPG membranes (Fig. 3*A*), which mimic *E. coli* lipid membranes (49). Since HALO-F caused greatly increased dye release in comparison with the other HALO peptides, and because D-HALO-rev, HALO-P8, and HALO-F have such dissimilar toxicity to either erythrocytes or lung fibroblasts, we prepared a further peptide containing both proline and phenylalanine motifs and composed of entirely D-amino acids (D-HALO-P8F-rev). This peptide had intermediate dye release activity when challenging, for example, POPE/POPG vesicles (Fig. 3*A*), indicating that the higher pore-forming activity of a phenylalanine-rich peptide could be reduced by either incorporating a proline kink or by altering the chirality of the peptide or through a combination of both. Notably, the effect of D-HALO-P8F-rev on bacteria at or around the MIC is to deform the cell surface through membrane blebs or invaginations of the cell surface, yet cell leakage, which would imply pore formation, is not observed until bacteria are challenged with a high concentration of peptide (4–8 times MIC).

Dye release from neutral liposomes containing cholesterol, which simulate the plasma membrane of normal fibroblasts, is minimal when challenged by any of the HALO peptides (Fig. 3, *B* and *C*). In the absence of anionic POPS, only the two peptides containing phenylalanine residues are capable of causing any measurable dye release and then only at rather low levels (Fig. 3*B*). When POPS is included in the membranes, the activity of all of the peptides is slightly enhanced (Fig. 2*C*). Dye release is measurable for all peptides, with the phenylalanine- and proline-enriched peptides showing the greatest activity. HALO-F causes the release of more than twice as much dye as its nearest rival.

Lipid Disruption—A recent molecular dynamics study of the behavior of cationic amphipathic antimicrobial peptides in model membranes has linked the localized disruption of lipids, and in particular the lipid acyl chains, to the formation of disordered toroidal pores (4). An experimental view of this effect can be obtained by acquiring wide line ^{2}H echo spectra (32) of the lipid mixes in the absence and presence of peptide. This approach gives a detailed picture of the effect of the peptides on the lipid acyl chains in model membranes. HALO peptides are added at 1.7 or 2 mol % with respect to the phospholipid content of the model membranes, since this peptide/lipid ratio represents a situation where considerable dye release and hence pore formation occurs when the action of pleurocidin on model membranes was studied (45) and is close to that used in the molecular modeling study (4). The spectra obtained are shown in Fig. 4 or are available as supplemental material, whereas the data are presented in the form of either smoothed or averaged order parameters for the respective acyl chains, calculated relative to peptide-free membranes.

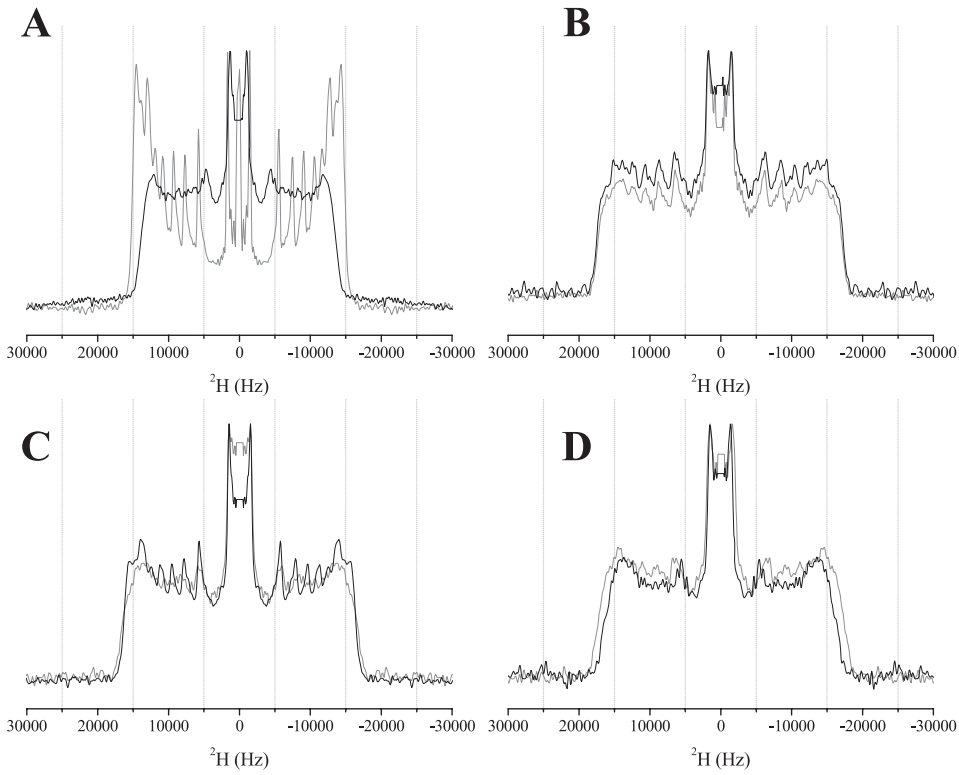

FIGURE 4. **Comparison of the membrane-disordering effect of HALO on deuterium-labeled lipid-containing membranes of varying composition.** Solid echo ^{2}H spectra recorded on a Bruker Avance 300 spectrometer at 310 K are shown for POPE/POPG-d31 (*A*), POPC-d31/cholesterol (*B*), POPC/POPC-d31/POPS/cholesterol (*C*), and POPC/POPS-d31/cholesterol (*D*). HALO was added at 2 mol % (*A* and *B*) or 1.7 mol % (*C* and *D*).

The addition of HALO and its derivatives to membranes composed of POPE/POPG-d31 causes a noticeable reduction in the quadrupolar splittings observed for labeled sites throughout the acyl chain of the anionic lipid (Fig. 4*A*). Calculation of the smoothed order parameter profiles for the lipid chain reveals that the order is markedly reduced and proportionally greatest in the lower part of the chain, corresponding to the hydrophobic center of the lipid bilayer (Fig. 5*A*). Average chain order parameters, calculated for either the full-length or the lower part of the acyl chains, indicate that the disruption in chain order is similar for each of the five HALO peptides tested, with only small variations from one peptide to another (Fig. 5, *E* and *F*).

Considering the differing toxicity of HALO, HALO-P8, and HALO-F, these three peptides were also tested for their effects on membranes simulating eukaryote plasma membranes (Fig. 5, *B–D*). To this end, similar experiments were performed on membranes composed of POPC/cholesterol (Fig. 4*B*) or POPC/POPS/cholesterol (Fig. 4, *C* and *D*), where either POPC-d31 or POPS-d31 was included as the labeled lipid. The order parameter profiles show that in the absence of an anionic lipid in the membrane, very little reduction of the quadrupolar splittings is induced by the addition of the three peptides (Fig. 5*B*). The binding of cationic peptides to model membranes is strongly affected by surface charge, and cationic peptides appear to interact far less strongly with neutral membranes (3). However, the binding of such peptides to cell surfaces has been shown to be mediated by heparan sulfate groups (50); hence, an anionic model membrane, which enhances peptide binding, may also provide useful information about how HALO peptides may behave in normal eukaryote plasma membranes once bound. When the anionic lipid POPS is included in the membrane, notable disordering of the lipid acyl chains occurs for both anionic and zwitterionic labeled lipids (Fig. 5, *C* and *D*). Although in general, for all three peptides, the anionic lipid is more strongly disordered, notable differences between the activities of the three peptides can be discerned. HALO-P8 appears to be rather less effective at disordering the zwitterionic POPC-d31 in mixed POPC/POPS/cholesterol membranes than either HALO or HALO-F (Fig. 5*E*), most notably in the hydrophobic core region of the acyl chain (Fig. 5*F*). Within this region of the membrane, the activity of HALO-P8 against anionic POPS-d31 is, however, comparable with that of HALO, whereas the activity of HALO-F is greater than either peptide (Fig. 5*F*).

Orientation of Peptides in Model Membranes—The preparation of samples containing HALO simultaneously labeled with ^{15}N at positions Leu-12 and Leu-14 and aligned on glass plates and the subsequent measurement of the static proton-decoupled ^{15}N CP spectrum allow an accurate determination of the value of the anisotropic chemical shift (Fig. 6*A*). This parameter correlates strongly with the membrane topology of helical polypeptides, with chemical shifts $<$100 ppm being indicative of in-plane alignments, whereas values in the 200 ppm region correspond to transmembrane orientations (17, 51). Unaligned peptides would give rise to very broad spectra ($\sim$170 ppm) representing the powder pattern of the ^{15}N chemical shift anisotropy (51). A value of 73.5 ppm indicates that the long axis of the peptide helix is oriented parallel to the membrane surface, as expected from the design considerations. The peak is a result of the contributions from two residues, but analysis by a peak fitting routine did not show any indication of shoulders or multiple components, indicating that the two labeled sites in the peptide adopt a similar orientation. The resonance full width at half height of 17.2 ppm, however, constitutes a spread of orientations and is a reflection of the disruption of the POPE/POPG membrane induced by the peptide. Previous work has shown that the presence of positively charged residues, positioned at the center of a helical amphipathic peptide, is not tolerated in the hydrophobic core of the membrane, causing the peptide to adopt a surface rather than a trans-membrane alignment (17). This hypothesis was confirmed by performing similar experiments with LAH4-L1-IP (Fig. 6*B*) and KALP (35) (available as supplemental material), which both have a nominal charge of +5 at neutral pH, to confirm that moving the charged residues

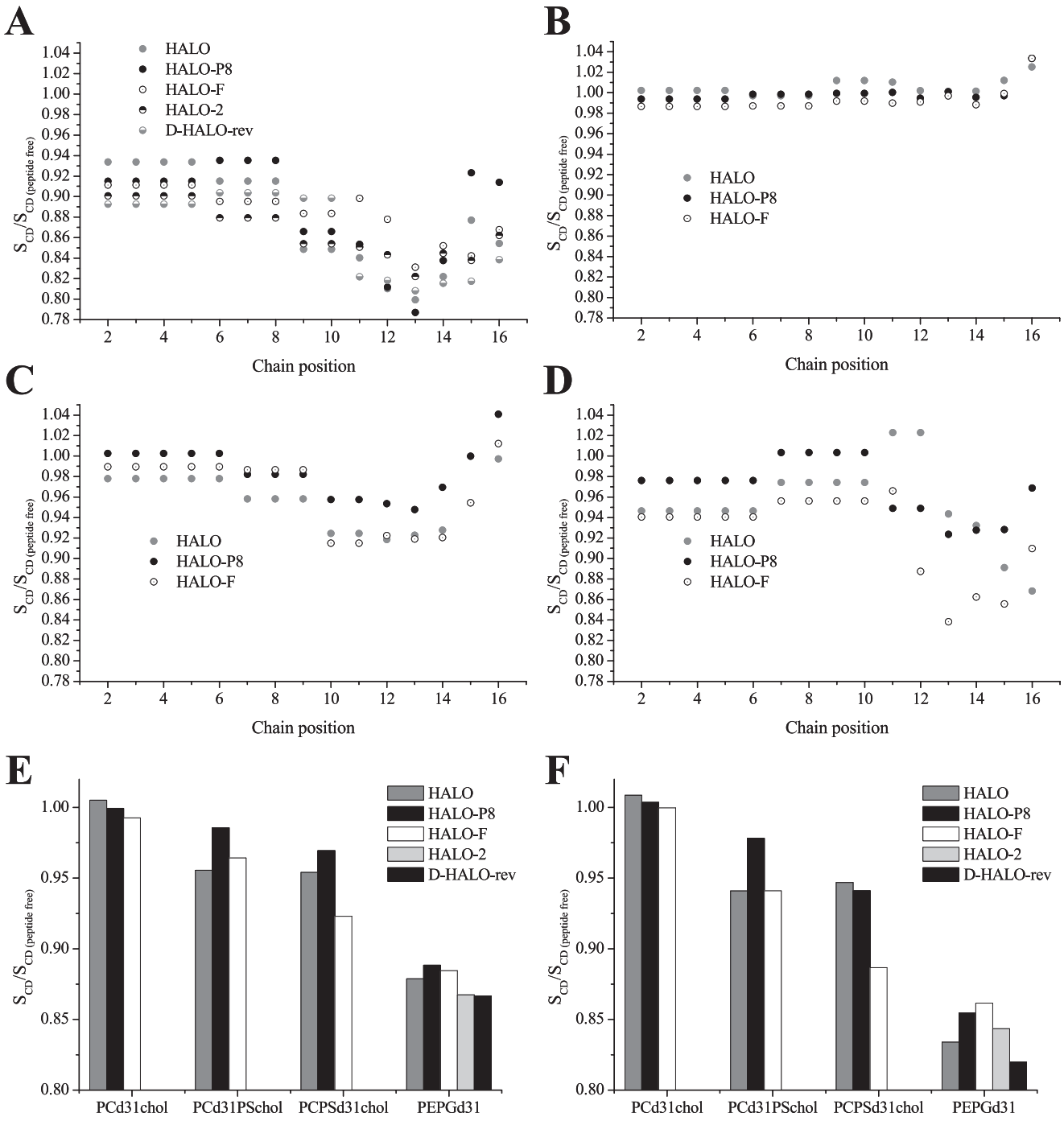

FIGURE 5. **The effect of adding HALO, HALO-P8, and HALO-F to liposomes containing POPE/POPG-d31 (*A*), POPC-d31/cholesterol (*B*), POPC-d31/POPS/cholesterol (*C*), or POPC/POPS-d31/cholesterol (*D*), as observed by acquiring ^{2}H spectra of the deuterium-labeled anionic POPG-d31 or POPS-d31 or zwitterionic POPC-d31.** Smoothed order parameters obtained for spectra obtained when incubated with either 2 (*A* and *B*) or 1.7 (*C* and *D*) mol % peptide are shown calculated relative to profiles for the corresponding peptide-free liposomes. HALO-2 and D-HALO-rev were also added to POPE/POPG-d31 liposomes (*A*). Spectra were recorded on a Bruker Avance 300 spectrometer at 310 K. The average chain order parameters are compared over the full length (*E*) or lower six carbons (*F*) of the lipid acyl chain.

from the termini to the center of the peptide results in an in-plane orientation of the peptide. Sequences related to KALP have been shown to adopt a trans-membrane orientation in a range of model membranes (52), and this orientation is also observed here for KALP. For LAH4-L1-IP, two resonances can be resolved (Fig. 6*B*), reflecting the greater difference in alignments of two residues that are adjacent to each other (Leu-13 and -14) than two separated residues (Leu-12 and -14), as per the HALO family. Further aligned samples were prepared containing either HALO-F or HALO-P8. These peptides were labeled in the same positions as HALO, but HALO-P8 carried an additional label at position Leu-5. The spectra obtained either in POPE/POPG (Fig. 6*A*) or POPC/cholesterol (Fig. 6*B*) membranes indicate that all of the peptides adopt a surface

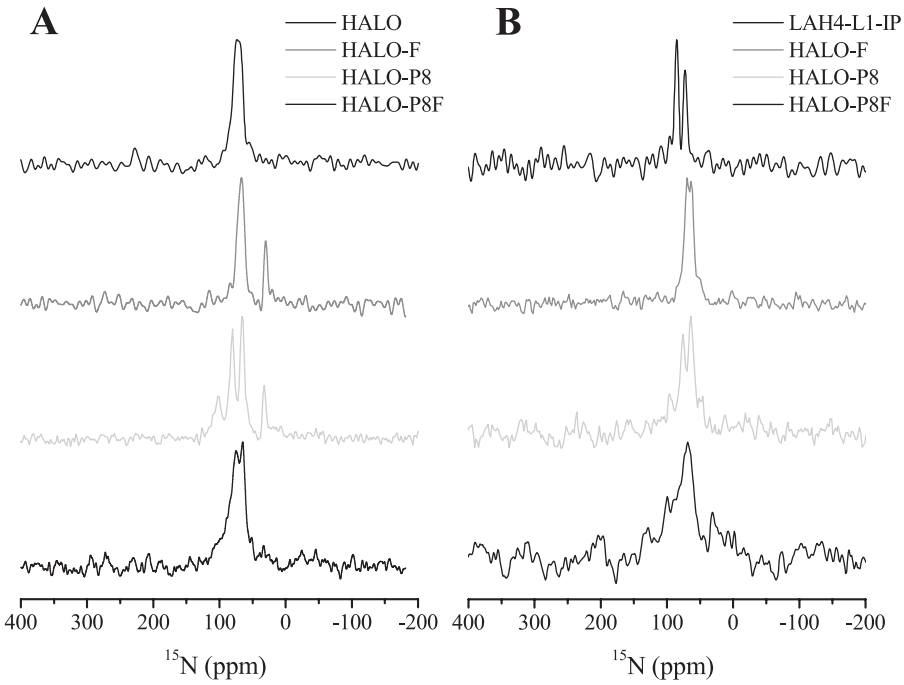

FIGURE 6. **Proton-decoupled static oriented ^{15}N solid state NMR spectra of 2.5 mol % HALO peptides in aligned POPE/POPG (75:25) (*A*) or POPC (LAH4-L1-IP) or POPC/cholesterol (100:30) (HALO-F, HALO-P8, and HALO-P8F) (*B*) membranes indicating a surface alignment of the peptide.** HALO, HALO-F, HALO-P8, and HALO-P8F all carry ^{15}N labels at positions 12 and 14, whereas HALO-P8 and HALO-P8F carry an additional label at position 5. LAH4-L1-IP is labeled at positions 13 and 14. The membranes remain aligned and intact, as confirmed by the ^{31}P NMR spectrum of the same samples (*e.g.* see supplemental material).

alignment and that no large shifts of the major resonances are observed between HALO and its derivatives or when the lipid environment is changed. Therefore, modification of the HALO peptide, by incorporating phenylalanine or proline, does not cause the peptide to tilt dramatically away from the surface alignment adopted by HALO itself, further confirmation that the placement of the positively charged residues is the main determinant of alignment for this class of peptides. For HALO-P8, however, a further, less intense but broader resonance is observed at 102.4 and 95.9 ppm in POPE/POPG or POPC/cholesterol, respectively. Assuming that the region around the additional label at Leu-5 remains helical, this indicates that the additional label is in a section of the peptide that undergoes motional averaging or adopts an alternate orientation to the remainder of the peptide. Additional sharp resonances are observed around 30 ppm for two peptides in the presence of POPE/POPG (Fig. 6*A*). These resonances are located upfield of the region where ^{15}N-leucine amide resonances are expected and may be ascribed to natural abundance ^{15}N in the lipid headgroups, which may appear according to slight variations in sample hydration during application of radio frequency pulses.

DISCUSSION

The designed histidine-rich antimicrobial peptides comprising the HALO family are distinct from their parent peptide, LAH4-L1, in terms of both their biophysical behavior in the presence of model lipid membranes and their antimicrobial activities. At neutral pH, the HALO peptides adopt a surface alignment and strongly destabilize the lipid acyl chains in mixed POPE/POPG-d31 membranes, whereas the peptides are potent broad spectrum antibacterial agents against bacteria, such as *E. coli*, *S. aureus*, and *P. aeruginosa*. LAH4-L1 and other related peptides are also interesting antibiotics (15), but at neutral pH, far greater quantities are required to inhibit growth of *P. aeruginosa*, for example, which is essentially resistant to such peptides in the concentration range that might be clinically acceptable. LAH4 adopts a trans-membrane orientation at neutral pH (17), and peptides from this family induce only minimal disruption of lipid acyl chain order under such conditions (15, 28). Therefore, it seems clear that the in-plane orientation adopted by the HALO peptides is essential for their higher antimicrobial activity, relative to the parent LAH4-L1. A surface orientation has been described for a number of antimicrobial peptides derived from natural sources (8, 11–13), and a model for pore formation induced by cationic amphipathic peptides maintaining such an alignment has been described using an in silico molecular modeling approach (4). This model indicates that a surface-aligned peptide, when reaching a similar peptide/lipid ratio as used in the present study, induces a local disruption of lipid acyl chains, and a "disordered toroidal pore" forms, where the peptides maintain an alignment approximately parallel to the membrane surface. During this process, the membrane is disrupted locally, and this allows the peptides to enter the cell interior. Antimicrobial peptides can have pore forming or intracellular targeting bactericidal strategies (2), whereas some peptides, such as pleurocidin, have been identified as being capable of both (9, 10). In the present study, we have designed cationic amphipathic antimicrobial peptides that deform the bacterial cell surface of both Gram-positive and Gram-negative bacteria at or around their MIC, implicating membrane-localized events in the inhibitory and bactericidal mechanisms. Only at peptide concentrations considerably in excess of the MIC, however, do the cell contents appear to be released. In agreement with this, evidence from biophysical techniques suggests that these designed peptides can disrupt the acyl chains of anionic phospholipids and be potent bactericidal antimicrobial agents without forming pores big enough to release calcein from the vesicle interior. Furthermore, small alterations in primary sequence at its extreme N terminus, such as adding two phenylalanine residues, can confer greatly increased pore-forming activity on an amphipathic peptide without affecting either its antimicrobial potency or its ability to disorder lipids in model membranes. Taken together, these observations indicate that the activity of the HALO peptides, at or around their MIC, may not be dependent on pore formation alone and that such activity may only be incidental to

other antibacterial mechanisms. The ability of the peptides to disrupt lipid acyl chains does, however, appear to be linked to the antibacterial potency, and therefore the ability of HALO and its variants to enter bacteria may be closely linked to the ability of the peptide to induce localized lipid disruption.

Interestingly, HALO and its derivatives possess very different levels of toxicity to human cells, whereas the pattern of toxicity is also different when comparing lung fibroblasts and erythrocytes. Understanding the relevant differences between the two cell types in combination with the data provided by the biophysical aspect of the present study allows us to identify not only how cationic amphipathic helical antimicrobial peptides function but also, in this case, how the peptides can be altered to acquire either reduced or more selective toxicity relevant to the intended application. Erythrocytes differ from many other eukaryote cells in that they have no nucleus or internal membranes, and, although it can be induced by certain drugs (53), endocytosis does not normally occur. Although the underlying mechanism of the antibacterial activity of cationic helical peptides has been studied quite extensively, the means by which such peptides are toxic to eukaryote cells and, in particular, cancer cells has received less attention. Recently, however, peptides such as lactoferricin have been investigated as potential anti-cancer agents, and it has been shown that this peptide enters neuroblastoma cells and depolarizes mitochondrial membranes (54). This initiates a number of necrotic and apoptotic processes, but ultimately, the main events leading to cell death are the destabilization of the cell membrane and the collapse of the outer and inner mitochondrial membranes. Our observations and biophysical study lend strong support for this mechanism. D-HALO-rev, for example, is the least toxic of the peptides to erythrocytes but is the most toxic toward either normal or transformed fibroblasts. In addition, D-HALO-rev has the poorest pore-forming activity across the three model membranes but is nonetheless capable of disordering lipid acyl chains in the POPE/POPG-d31 model membranes. Internal membranes, such as the inner and outer mitochondrial membranes, have far lower cholesterol content than the plasma membrane (55), making them more vulnerable to the action of cationic helical peptides, whose lipid-disrupting and pore-forming abilities are strongly modulated by the presence of sterols in model membranes (14). In contrast, HALO-F is highly toxic to both erythrocytes and fibroblasts when compared with the original HALO peptide. In addition, HALO-F causes dye release from model membranes that is far greater than that of any of the other HALO peptides tested and was the only peptide tested to cause acyl chain disordering in neutral cholesterol-rich membranes. It is likely that this behavior underlies the extremely high toxicity observed for both human cell types that were challenged.

Cationic helical peptides, such as NK-2, dermaseptin S4, and its acylated derivatives, have also been shown to have antiparasitic activity in culture (56–60). The less potent of these are hemolytic at their active concentrations, although erythrocytes infected with *P. falciparum* appear often to be more susceptible to lysis than noninfected host cells (56–58). More potent peptides, including acylated derivatives (58, 59) and, in particular, peptide analogues (60), are active at concentrations far below that required for erythrocyte lysis, and such peptides have been shown to be localized at the parasite membrane within infected erythrocytes (56, 59). In the present study, the antiplasmodial activity of, in particular, D-HALO-rev indicates that histidine-rich peptides can be designed that can also enter *P. falciparum*-infected erythrocytes at sublytic concentrations and kill the parasite. The mechanism for this antiplasmodial activity is, as yet, unclear. However, again, important differences in the membrane composition of *Plasmodium* spp. and the cells that they have infected are predicted to enhance the activity of designed antiplasmodial peptides. One major difference is that *Plasmodium* plasma membranes also have an extremely low cholesterol content (61). Furthermore, both exposure of phosphatidylserine at the external surface of the erythrocyte plasma membrane (40, 56) and increased membrane fluidity and disorder, accompanying an increase in the proportion of unsaturated lipid acyl chains in the erythrocyte membrane phospholipids and a slight reduction of the cholesterol content (62–65), have been demonstrated postinfection. In contrast, healthy erythrocyte membranes retain asymmetry, and phosphatidylserine is not presented at the external surface prior to a pathological stimulus (40). Therefore, as with the internal membranes discussed above, the *Plasmodium* plasma membrane would be far more susceptible to the action of the HALO peptides than the membranes of its uninfected host cells, since the action of cationic α-helical peptides is closely related to the presence of negatively charged phospholipids and disorder in the membrane (14).

As mentioned above, interest has been growing in the ability of cationic helical peptides to display selective toxicity toward transformed cells over normal ones. The basis for this selectivity is proposed to be the presence of anionic lipids at the external surface of the plasma membrane of transformed cells (36–40), and this has been demonstrated to be the case for the action of the NK-2 peptide on cancer cells presenting phosphatidylserine (66). Consistent with this, the HALO peptides display greater toxicity toward MRC5 fibroblasts that have been transformed with the SV40 virus (MRC5-V2). Incorporating a proline residue at position 8 in the HALO sequence reduces toxicity toward both cell types but enhances the selectivity of the peptide toward the MRC5-V2 cells in the presence of serum. Although other studies have produced peptides with greater specificity and activity toward cancer cell lines (38, 66, 67), the potential to tune the selectivity of a membrane active peptide by carefully incorporating just one proline residue is rather attractive. Incorporation of a proline residue has already been shown to reduce the toxicity of piscidin-1 to erythrocytes, whereas the peptide retained its antimicrobial potency (31). Here we obtain similar results with the HALO peptides but also demonstrate that the incorporation of a proline, in combination with D-amino acids and the phenylalanine motif, allows a peptide to be produced that has low toxicity to erythrocytes and reduced toxicity toward fibroblasts yet remains a robust antibiotic. The deuterium NMR data suggests that the incorporation of a proline residue can lead to a greater reduction of the lipid acyl chain disordering of zwitterionic POPC lipids than anionic POPS lipids when HALO peptides insert into the membrane. This could be a result of a reduction in the length of the helical

segment in the peptide, or, since we and others have shown that the angle subtended by the charged segment in the helical wheel is also important for selection of anionic over zwitterionic lipids (26–29), the proline-induced kink and concomitant conformation flexibility could allow modulation of the effective charged angle and afford selectivity through this alternate route. The relative contributions of these effects could provide the basis for incorporating extensive selectivity in the design of future generations of cationic helical membrane active peptides.

Acknowledgments—A. J. M. thanks Gérard Nullans (U575) for mass spectrometry analysis, Claire Gasnier (U575) for initial antibacterial tests, and Roland Bury (U666) for scanning electron microscopy experiments. ISIS is acknowledged for hosting the laboratory.

REFERENCES

1. Hancock, R. E. W., and Sahl, H-G. (2006) *Nat. Biotechnol.* **24,** 1551–1557
2. Brogden, K. A. (2005) *Nat. Rev. Microbiol.* **3,** 238–250
3. Bechinger, B. (2004) *Crit. Rev. Plant Sci.* **23,** 271–292
4. Leontiadou, H., Mark, A. E., and Marrink, S. J. (2006) *J. Am. Chem. Soc.* **128,** 12156–12161
5. Yandek, L. E., Pokorny, A., Florén, A., Knoelke, K., Langel, Ü., and Almeida, P. F. F. (2007) *Biophys. J.* **92,** 2434–2444
6. Ramamoorthy, A., Thennarasu, S., Lee, D-K., Tan, A., and Maloy, L. (2006) *Biophys. J.* **91,** 206–216
7. Matsuzaki, K., Murase, O., Fujii, N., and Miyajima, K. (1995) *Biochemistry* **34,** 6521–6526
8. Mason, A. J., Chotimah, I. N. H., Bertani, P., and Bechinger, B. (2006) *Mol. Membr. Biol.* **23,** 185–194
9. Saint, N., Cadiou, H., Bessin, Y., and Molle, G. (2002) *Biochim. Biophys. Acta* **1564,** 359–364
10. Patrzykat, A., Friedrich, C. L., Zhang, L., Mendoza, V., and Hancock, R. E. (2002) *Antimicrob. Agents Chemother.* **46,** 605–614
11. Bechinger, B., Zasloff, M., and Opella, S. J. (1993) *Protein Sci.* **2,** 2077–2084
12. Chekmenev, E. Y., Vollmar, B. S., Forseth, K. T., Manion, M. N., Jones, S. M., Wagner, T. J., Endicott, R. M., Kyriss, B. P., Homem, L. M., Pate, M., He, J., Raines, J., Gor'kov, P. L., Brey, W. W., Mitchell, D. J., Auman, A. J., Ellard-Ivey M. J., Blazyk, J., and Cotton, M. (2006) *Biochim. Biophys. Acta* **1758,** 1359–1372
13. Mason A. J., Bertani, P., Moulay, G., Marquette, A., Perrone, B., Drake, A. F., Kichler, A., and Bechinger, B. (2007) *Biochemistry* **46,** 15175–15187
14. Mason, A. J., Marquette, A., and Bechinger, B. (2007) *Biophys. J.* **93,** 4289–4299
15. Mason, A. J., Gasnier, C., Kichler, A., Prévost, G., Aunis, D., Metz-Boutigue, M-H., and Bechinger, B. (2006) *Antimicrob. Agents Chemother.* **50,** 3305–3311
16. Vogt, T. C. B., and Bechinger, B. (1999) *J. Biol. Chem.* **274,** 29115–29121
17. Bechinger, B. (1996) *J. Mol. Biol.* **263,** 768–775
18. Mason, A. J., Bechinger, B., and Kichler, A. (2007) *Mini Rev. Med. Chem.* **7,** 491–497
19. Hallock, K. J., Henzler-Wildman, K., Lee, D-K., and Ramamoorthy, A. (2002) *Biophys. J.* **82,** 2499–2503
20. Davis, J. H. (1983) *Biochim. Biophys. Acta* **737,** 117–171
21. Schäfer, H., Mädler, B., and Volke, F. (1995) *J. Magn. Reson.* **116,** 145–149
22. Sternin, E., Bloom, M., and MacKay, A. L. (1983) *J. Magn. Reson.* **55,** 274–282
23. Seelig, A., and Seelig, J. (1974) *Biochemistry* **13,** 4839–4845
24. Cranmer, S. L., Magowan, C., Liang, J., Coppel, R. L., and Cooke, B. M. (1997) *Trans. R. Soc. Trop. Med. Hyg.* **91,** 363–365
25. Doderer, C., Heschung, A., Guntz, P., Cazenave, J. P., Hansmann, Y., Senegas, A., Pfaff, A. W., Abdelrahman, T., and Candolfi, E. (2007) *Malar. J.* **6,** 19
26. Alley, M. C., Scudiero, D. A., Monks, A., Hursey, M. L., Czerwinski, M. J., Fine, D. L., Abbott, B. J., Mayo, J. G., Shoemaker, R. H., and Boyd, M. R. (1988) *Cancer Res.* **48,** 589–601
27. Tytler, E. M., Segresi, J. P., Epand, R. M., Nie, S-Q., Epand, R. F., Mishra, V. K., Venkatachalapathi, Y. V., and Anantharamaiah, G. M. (1993) *J. Biol. Chem.* **268,** 22122–22118
28. Mason, A. J., Martinez, A., Glaubitz, C., Danos, O., Kichler, A., and Bechinger, B. (2006) *FASEB J.* **20,** 320–322
29. Wieprecht, T., Dathe, M., Epand, R. M., Beyermann, M., Krause, E., Maloy, W. L., MacDonald, D. L., and Bienert, M. (1997) *Biochemistry* **36,** 12869–12880
30. Jin, Y., Hammer, J., Pate, M., Zhang, Y., Zhu, F., Zmuda, E., and Blazyk, J. (2005) *Antimicrob. Agents Chemother.* **49,** 4957–4964
31. Lee, S-A., Kim, Y. K., Lim, S. S., Zhu, W. L., Ko, H., Shin, S. Y., Hahm, K-S., and Kim, Y. (2007) *Biochemistry* **46,** 3653–3663
32. Nishikawa, M., and Ogawa, K. (2004) *FEMS Microbiol. Lett.* **239,** 255–259
33. Hong, S. Y., Oh J. E., and Lee, K-H. (1999) *Biochem. Pharmacol.* **58,** 1775–1780
34. Chen, Y., Mant, C. T., Farmer, S. W., Hancock, R. E. W., Vasil, M. L., and Hodges, R. S. (2005) *J. Biol. Chem.* **280,** 12316–12329
35. Killian, J. A., Salemink, I. de Planque, M. R. R., Lindblom, G., Koeppe, R. E., II, and Greathouse, D. V. (1996) *Biochemistry* **35,** 1037–1045
36. Rinaldi, A. C., Mangoni, M. L., Rufo. A., Luzi, C., Barra, D., Zhao, H., Kinnunen, P. K., Bozzi, A., Di Giulio, A., and Simmaco, M. (2002) *Biochem. J.* **22,** 91–100
37. Shin, S. Y., Lee, S. H., Yang, S. T., Park, E. J., Lee, D. G., Lee, M. K., Eom, S. H., Song, W. K., Kim, Y., Hahm, K. S., and Kim, J. I. (2001) *J. Pept. Res.* **58,** 504–514
38. Yang, N., Strøm, M. B., Mekonned, S. M., Svendsen, J. S., and Rekdal, Ø. (2004) *J. Peptide Sci.* **10,** 37–46
39. Chen, H. M., Wang, W., Smith, D., and Chan, S. C. (1997) *Biochim. Biophys. Acta* **1336,** 171–179
40. Zwaal, R. F. A., Comfurius, P., and Bevers, E. M. (2005) *Cell. Mol. Life Sci.* **62,** 971–988
41. Utsugi, T., Schroit, A. J., Connor, J., Bucana, C. D., and Fidler, I. J. (1991) *Cancer Res.* **51,** 3062–3066
42. Huschtscha, L. I., and Holliday, R. (1983) *J. Cell Sci.* **63,** 77–99
43. Blazyk, J., Wiegand, R., Klein, J., Hammer, J., Epand, R. M., Epand, R. F., Maloy, W. L., and Kari, U. P. (2001) *J. Biol. Chem.* **276,** 27899–27906
44. Bechinger, B., and Lohner, K. (2006) *Biochim. Biophys. Acta* **1758,** 1529–1539
45. Yoshida, K., Mukai, Y., Niidome, T., Takashi, C., Tokunaga, Y., Hatakeyama, T., and Aoyagi, H. (2001) *J. Peptide Res.* **57,** 119–126
46. Sreerama, N., and Woody, R. W. (2000) *Anal. Biochem.* **287,** 252–260
47. Rohl, C. A., Chakrabartty, A., and Baldwin, R. L. (1996) *Protein Sci.* **5,** 2623–2637
48. Marquette, A., Mason, A. J., and Bechinger, B. (2008) *J. Pept. Sci.* **14,** 488–495
49. Morein, S., Andersson, A-S., Rilfors, L., and Lindblom, G. (1996) *J. Biol. Chem.* **271,** 6801–6809
50. Goncalves, E., Kitas, E., and Seelig, J. (2005) *Biochemistry* **44,** 2692–2702
51. Bechinger, B., and Sizun, C. (2003) *Concepts Magn. Reson.* **18A,** 130–145
52. Harzer, U., and Bechinger, B. (2000) *Biochemistry* **39,** 13106–13114
53. Ben-Bassat, I., Bensch, K. G., and Schrier, S. L. (1972) *J. Clin. Invest.* **51,** 1833–1844
54. Eliassen, L. T., Berge, G., Leknessund, A., Wikman, M., Lindin, I., Løkke, C., Ponthan, F., Johnsen, J. I., Sveinbjørssen, B., Kogner, P., Flægstad, T., and Rekdal, Ø. (2006) *Int. J. Cancer* **119,** 493–500
55. Daum, G., and Vance, J. E. (1997) *Prog. Lipid Res.* **36,** 103–130
56. Gelhaus, C., Jacobs, T., Andrä, J., and Leippe, M. (2008) *Antimicrob. Agents Chemother.* **52,** 1713–20
57. Krugliak, M., Feder, R., Zolotarev, V. Y., Gaidukov, L., Dagan, A., Ginsburg, H., and Mor, A. (2000) *Antimicrob. Agents Chemother.* **44,** 2442–2451
58. Dagan, A., Efron, L., Gaidukov, L., Mor, A., and Ginsburg, H. (2002) *Antimicrob. Agents Chemother.* **46,** 1059–1066
59. Efron, L., Dagan, A., Gaidukov, L., Ginsburg, H., and Mor, A. (2002) *J. Biol. Chem.* **277,** 24067–24072

60. Radzishevsky, I., Krugliak, M., Ginsburg, H., and Mor, A. (2007) *Antimicrob. Agents Chemother.* **51,** 1753–1759
61. Sherman, I. W. (1979) *Microbiol. Rev.* **43,** 453–495
62. Vial, H. J., and Ancelin, M. L. (1992) *Subcell. Biochem.* **18,** 259–306
63. Maguire, P. A., and Sherman I. W. (1990) *Mol. Biochem. Parasitol.* **38,** 105–112
64. Sherman, I. W., and Greenan, J. R. (1984) *Trans. R. Soc. Trop. Med. Hyg.* **78,** 641–644
65. Hsiao, L. L., Howard, R. J., Aikawa, M., and Taraschi, T. F. (1991) *Biochem. J.* **274,** 121–132
66. Schröder-Borm, H., Bakalova, R., and Andrä, J. (2005) *FEBS Lett.* **579,** 6128–6134
67. Yang, N., Stensen, W., Svendsen, J. S., and Rekdal, Ø. (2002) *J. Peptide Res.* **60,** 187–197